Spectrometric determination of the rest mass of the electron and the speed of light

Alexander Nie and Mobolaji Williams
Harvard University, 77 Massachusetts Ave., Cambridge, MA 02138
(Dated: April 7, 2016)

In this experiment, we measured the rest mass of the electron and the speed of light by making independent measurements of electron velocity and momentum and then fitting these measurements to the relativistic relationship between velocity and momentum. The electrons were produced with a Sr-90 source and the kinematics of the electrons were controlled and measured with a spectrometer. With both speed of light c and electron mass m as fitting parameters, we found $c = (3.04 \pm 0.09) \times 10^8$ m/s and $m = (9.5 \pm 0.4) \times 10^{-31}$ kg. With either parameter fixed to its currently best known physical value, we found for the other parameter $c = (2.96 \pm 0.2) \times 10^8$ m/s and $m = (9.3 \pm 0.06) \times 10^{-31}$ kg. These results encompass or are consistent with the best measured values of these constants, $c = 2.998 \times 10^8$ m/s and $m = 9.103 \times 10^{-31}$ kg.

I. INTRODUCTION

In 1897, J.J. Thompson measured the charge to mass ratio of the "corpuscles" which made up cathode rays. He thus firmly established the existence of the elementary particle we now call the electron [1]. Since then the electron has been an archetypical component of both theoretical and experimental modern physics. However, most of the electron's utility has been found in atomic and particle physics where models of the electron in various contexts led to the development of most of the early theoretical techniques of quantum mechanics and then the later extension of quantum physics to electrodynamics [2].

In this experiment, we studied the electron along the other branch of modern physics, and used the special relativistic relationship between velocity and momentum to determine the speed of light and the mass of the electron. We produced electrons with a Strontium-90 (Sr-90) source, after which electrons' trajectories curved through a magnetic field in the intervening space between two coaxial solenoids and then into an opposing electric field created by two plates of a capacitor. Past the capacitor plates, the electrons impinged on a Geiger detector and were registered as counts. By tuning and measuring the electric and magnetic fields during various parts of the electron's trajectory, we made independent measurements of the electron's momentum and velocity.

In Sec. II, we review the theory foundational to our velocity and momentum measurements. In Sec. III, we outline the experimental procedure and apparatus used to conduct these measurements. In Sec. IV, we present the main results and analysis of our experiment. In Sec. V, we discuss some interpretative challenges of the experiment, and in Sec. VI we present our conclusion. Ultimately, we found this spectrometric determination of the speed of light and the mass of electron was consistent with established experimental results.

II. THEORETICAL BACKGROUND

When a particle of mass m is moving at velocities v with speeds on the order of the speed of light c, it is necessary to replace the non-relativistic relationship between momentum and velocity (i.e., $p = mv$) with the special relativistic formula

$$p = \frac{mv}{\sqrt{1 - v^2/c^2}}, \tag{1}$$

where m is the rest mass of the particle, v is the particle's speed, p is the magnitude of the particle's momentum, and c is the speed of light. Eq.(1) was the equation this experiment sought to test. Specifically, we made independent measurements of an electron's momentum and velocity to determine the electron's rest mass and the speed of light given the p vs. v relationship in Eq.(1). Eq.(1) follows directly from the principles of relativity and can be derived by ensuring conservation of momentum is consistent with the time dilation effect predicted for inertial frames with a non-zero relative velocity [3].

A. Momentum from Magnetic Field

Electrons that eventually hit the Geiger detector first passed through a region with a magnetic field perpendicular to its plane of motion. For an electron moving in a magnetic field $\vec{B}$ (but zero electric field), the Lorentz force law states that the change in the electron's momentum follows

$$\frac{d\vec{p}}{dt} = -e\vec{v} \times \vec{B}, \tag{2}$$

where $\vec{p}$ is the electron's momentum, e is the electron's charge, and $\vec{v}$ is the electron's velocity. In such a scenario the magnetic field does no work on the electron and the electron moves along the arc of a circle. Therefore the momentum of the electron changes according to

$$\frac{d\vec{p}}{dt} = \vec{p} \times \vec{\omega} \tag{3}$$

where $\vec{\omega}$ is the angular velocity of the electron. Along a circular arc, the velocity $\vec{v}$ of an electron is $\vec{v} = R\hat{r} \times \vec{\omega}$, where R is the radius of the arc and $\hat{r}$ is a unit vector pointing radially away from the arc's circular center.

Given the forms of momentum and velocity applicable to a particle moving in a circular arc, our Lorentz force law can be written as

$$\vec{p} \times \vec{\omega} = -eR\,(\hat{r} \times \vec{\omega}) \times \vec{B} \tag{4}$$

Taking the magnitude of both sides and noting that the velocity, radial vector, and angular velocity are all perpendicular, we find

$$p = eRB, \tag{5}$$

where the scalar quantities are the magnitudes of the respective vectors in Eq.(4). With Eq.(5) we can determine the momentum of an electron traveling a long a circular arc of radius R in a magnetic field B.

B. Velocity from Crossed Electric and Magnetic Fields

After the electron passes through the magnetic-field only region, it passes through capacitor plates with a fixed potential difference. In this situation the electron electron's equation of motion is

$$\frac{d\vec{p}}{dt} = -e\vec{E} - e\vec{v} \times \vec{B}. \tag{6}$$

For electrons whose velocities were not changed upon entering the region of non-zero electric field, the right hand side of Eq.(6) is zero and the electron was able to pass through the field region without being disturbed/hitting the capacitor plates.

Thus, theoretically, given that v was fixed by the magnetic field (appropriately assuming a functional relationship between v and p), an electron would pass through the capacitor slits and register on the Geiger detector, only if the plates maintained a certain electric field in the space between them. That is, electrons passed through the capacitor plate slit if the electric field $\vec{E}$ satisfied

$$\vec{E} = -\vec{v} \times \vec{B}. \tag{7}$$

For this experiment, we were primarily interested in the speed of the electron, so taking the absolute value of both sides of Eq.(7) we find

$$v = \frac{E}{B}, \tag{8}$$

where scalar quantities are again the magnitudes of their corresponding vector ones.

In this experiment we swept over a range of electric field values and counted the number of hits we observed on our Geiger detector. Thus given Eq.(8), we expected to observe an increased count of electrons only for a specific electric field, and from this electric field we could determine the velocity of the electrons registered on the counter. Outside of velocity predictions, Eq.(7) was used to determine the polarity between the capacitor plates needed to achieve a force free region for the electrons.

III. APPARATUS AND PROCEDURE

In this section, we review the components and procedures we used to carry out the measurements in each round of data collection.

In a typical round of data collection, we measured the magnetic field in the spectrometer region and tuned it to a desired field value. For this field value, we then swept the voltage applied to the capacitor plates multiple times while recording the electron counts registered by the Geiger detector. We performed the sweep multiple times in order to obtain an aggregate electron count which was more consistent than one obtained through a single sweep. Throughout a single voltage sweep, the multimeter displayed the output voltage from the voltage divider. The multimeter's voltage was taken to be our main voltage measurement. After the final sweep for a particular magnetic field, the magnetic field was set to a new value and a new round of data collection began.

A. Sr-90 source

The decay spectrum of Sr-90 (Fig. 1) reveals that the number of electrons produced by the Sr-90 source varies as a function of the electron's energy. For our spectrometer setup, the energy of electrons that curved into the space between the capacitor plates depended on the magnetic field in the chamber. Thus, over the course of the experiment, as we swept the magnetic field from 225 gauss to 450 gauss, we were effectively sweeping the energy ranges of electrons permitted to enter the capacitor plates, and, by the Sr-90 decay spectrum Fig. 1, our number of electron counts varied with the particular magnetic field within the chamber. Such variation is apparent in the electron counts registered by the Geiger detector for various magnetic field values. Our applied magnetic field was bracketed by the range 225-450 gauss because below 225 gauss the electron signal was obscured by the noise and above 450 gauss the electrons selected by the magnetic field corresponded to an electric field larger than the High Voltage power supply could create.

B. Magnetic Field

The magnetic field for the experiment was created by current carrying wires. These wires were wrapped in two solenoidal configurations, one above and one below the

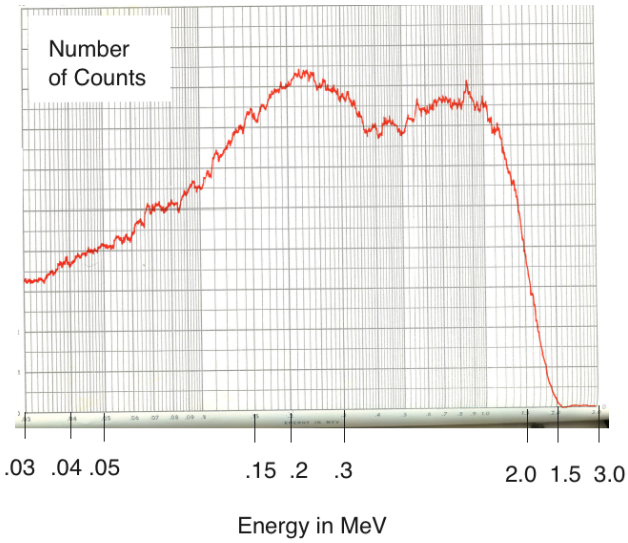

FIG. 1: Strontium-90/Ytrium-90 spectrum: The number of electrons produced by a Sr-90 source plotted as a function of the relativistic kinetic energy of those electrons. The exact number of counts is unimportant; only the peak locations are relevant. The peaks in the distribution occur at ~ 0.26 and ~ 0.87 MeV corresponding to electron velocities of $0.76c$ and $0.92c$ respectively, and given Eq.(5) and Eq.(1) corresponds to magnetic fields of 355 gauss and 770 gauss. Figure copied from Phys 191-r Lab guide.

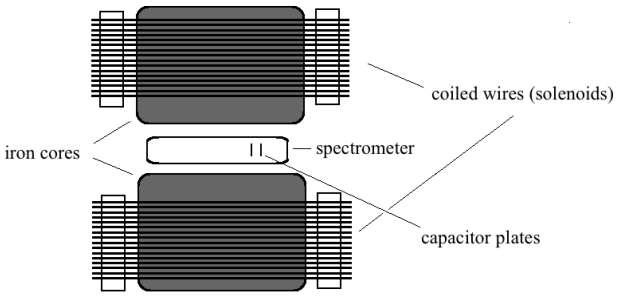

FIG. 2: Side-view cross section of experiment: Current carrying wires were wrapped in two solenoids both above and below the spectrometer. An iron core was at the center of each solenoid to increase the magnitude and promote the uniformity of the net magnetic field. Capacitor plates lie within spectrometer. Figure created by authors.

spectrometer setup as shown in Fig. 2. An iron core passed through the center of each solenoid, ending right above and right below the interior of the spectrometer. The core filled the entire cross section of the solenoid and was used to strengthen and promote uniformity of the magnetic field. Before each round of data collection, we measured the magnetic field using a gaussmeter (Bell 640 Incremental Gaussmeter), and tuned it with a current

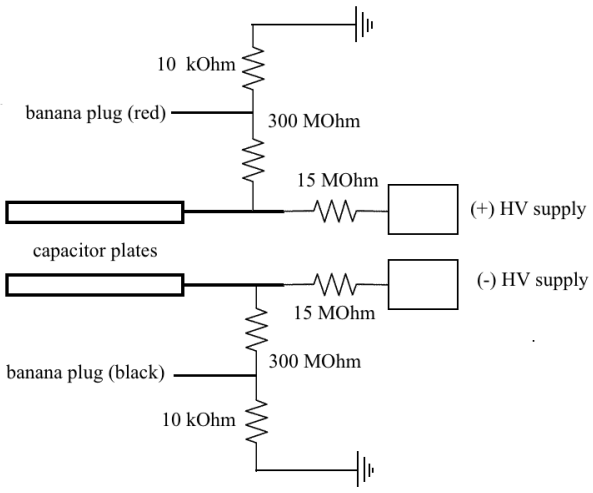

FIG. 3: Linear voltage divider: The linear voltage divider setup served as the main voltage divider for the experiment. It consisted of two identical circuit setups each connected to a terminal of the high voltage source and a capacitor plate, and the multimeter voltage was read across the red and black banana plugs. The 300 kΩ and 10 kΩ resistor values are approximate, and thus the exact voltage divider ratio had to be determined exactly before the experiment. The 15 MΩ resistors were used to limit the amount of current drawn from the high voltage source. Figure created by authors.

source (created by connecting a voltage source in parallel to a potentiometer).

C. High Voltage Power Source

For the experiment we swept our high voltage source from from 0 to ~ 8 kV (creating a potential difference of ~ 16 kV between the capacitor plates). The upper limit of this voltage range was constrained by the safety suggestions of the power source. The sweep was performed by a LABVIEW program and lasted 200 s. The precision of our voltage measurement varied inversely with our sweep time, but the time it took to complete the experiment varied proportionally with sweep time. We chose 200 s as a sweep time which could give us a desired voltage precision while allowing us to complete several trials of the experiment in the allotted class periods. A single sweep was defined as a single run, and, for each magnetic field setting, we performed five runs (whose electron counts were summed) to gather a single round of data.

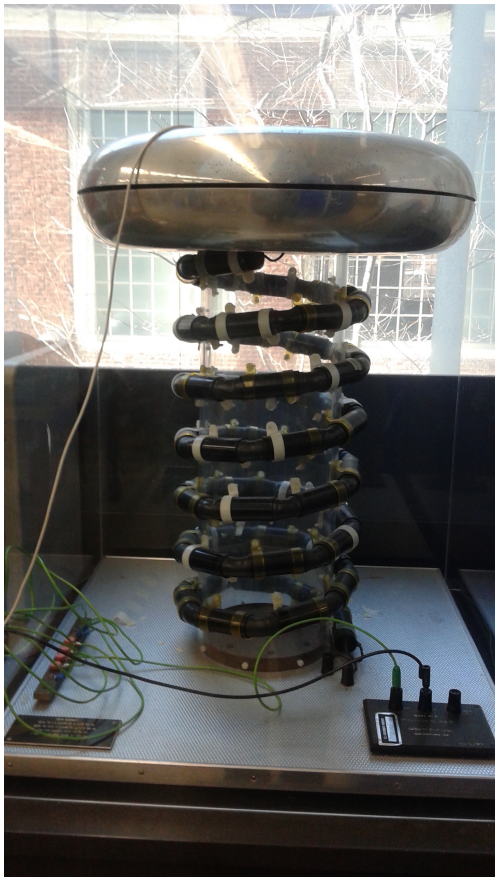

FIG. 4: Image of circular voltage divider: From a circuit diagram perspective, the circular voltage divider consisted of only one branch of the divider setup in Fig. 3. The resistors which comprised the main load (analogous to the 300 MΩ resistors in Fig. 3) were connected in series and arranged in a helix to conserve space. This voltage divider yielded a voltage-divider ratio of $V_{\text{out}}/V_{\text{in}} = 10^{-5}$ and was used to calibrate the ratios for each branch of the linear divider.

D. Voltage Divider

Presuming the validity of Eq.(1) and using Eq.(5) and Eq.(8), the magnitude of electric field needed to select an electron with velocity v is

$$E = \frac{mv^2}{eR}\frac{1}{\sqrt{1-v^2/c^2}}. \tag{9}$$

For an electric field E between the two capacitor plates a distance d apart, the resulting voltage difference between the plates is Ed. For our setup in Fig. 5, we then find that for speeds on the order of $0.5c$ (well within the relativistic regime), we need a voltage difference on the order of 3 kV, or about 1 kV (of opposite polarity) applied to each capacitor plate. These voltages were too high to read directly from a multimeter, so we instead used a voltage divider [4] to reduce the output voltage to the order of 10^2 mV, and we then read reduced voltage on the multimeter.

Specifically, we used two voltage divider setups. One, which we call the "linear" setup and is depicted as a circuit diagram in Fig. 3, had two terminals, and had an imprecise resistor ratio. An image of the other, which we called the "circular" setup and is shown in Fig. 4, had a single terminal, and had a precise resistor ratio of 10^{-5}. Because the linear divider had two terminals (one for each capacitor plate), it was used as the main voltage divider for the experiment. However, because the linear divider had an unknown voltage ratio, before the experiment we accurately determined the ratio using the circular voltage divider as a benchmark. The procedure was as follows. We applied the same input voltage to a single terminal of the linear divider and to the circular divider, and measured the corresponding output voltage for each divider. For example, for the positive terminal, the output voltage for each voltage divider was related to the input voltage V_{in}^+ according to

$$V_{\text{out, lin}}^+ = f_{\text{lin}}^+ V_{\text{in}}^+ \tag{10}$$

$$V_{\text{out, circ}}^+ = f_{\text{circ}} V_{\text{in}}^+, \tag{11}$$

where $V_{\text{out, lin/circ}}^+$ is the output voltage at the positive terminal for the linear/circular voltage divider and f_{lin}^+ is the voltage-divider ratio for the positive terminal of the linear divider. There is only one terminal for the circular voltage divider and hence it only has one corresponding voltage-divider ratio f_{circ}. With the output voltage for each divider known (as measured by the voltmeter) and the voltage ratio for the circular divider known, we were able to determine the voltage ratio for the linear divider through the equation

$$f_{\text{lin}}^+ = \frac{V_{\text{out, lin}}^+}{V_{\text{out, circ}}^+} f_{\text{circ}}. \tag{12}$$

By gradually ramping up the V_{in}^+ as output by the high voltage source, we performed multiple evaluations of f_{lin}^+ which were averaged to estimate the true voltage-divider ratio for each terminal. A similar methodology was used to determine the voltage-divider ratio for the negative terminal of the linear voltage divider.

E. Spectrometer and Pumps

The experiment took place within the chamber of a spectrometer. The components of the spectrometer most relevant to the experiment are shown in Fig. 5. From the figure we see that the Sr-90 electron source was placed within the magnetic field exclusive region. The released electrons followed a circular trajectory of radius R before entering into the space between the capacitors. This radius was determined from the geometry of the spectrometer as shown in Appendix A. Given that $\ell_1 = 55.6 \pm 0.2$ mm is the length of half of a chord of the circle, and

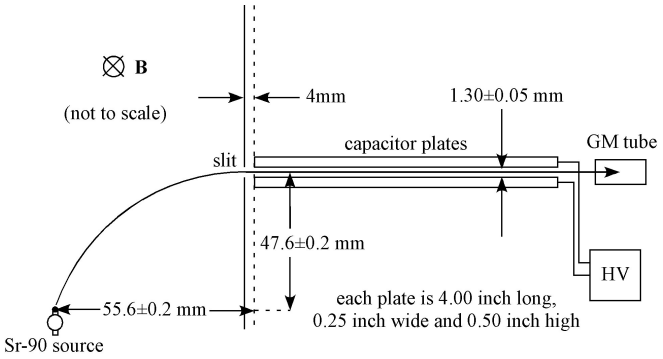

FIG. 5: Overhead view of spectrometer interior: Electrons leave the Sr-90 source and travel along a circular arc in a magnetic field exclusive region before entering the space between two capacitor plates. The electrons whose velocities satisfy Eq.(8) pass through the capacitor plates with no deflection and are incident on the Geiger-Mueller detector. Figure taken from experimental lab guide.

$\ell_2 = 47.6 \pm 0.2$ mm is the line bisecting that chord and running from the edge of the circle to the chord (but not to the circle's center), one can show that

$$R = \frac{\ell_1^2 + \ell_2^2}{2\ell_2} = 56.3 \pm 0.2 \text{ mm}. \tag{13}$$

This was the radius we used in our momentum determination defined by Eq.(5). The other important geometric quantity in the spectrometer was the distance between the capacitor plates, $d = 1.30 \pm 0.05$ mm. With this distance we were able to convert the voltage difference across the capacitors into an electric field.

Before we began collecting data, we created a high vacuum in the interior of the spectrometer using a two stage pump. First, we used a roughing pump to lower the pressure in the spectrometer interior to within $\mathcal{O}(10^{-2})$ Pa. Then, we used a turbo molecular pump to achieve pressures below $\mathcal{O}(10^{-4})$ Pa. A very low chamber-pressure is needed to reduce the number of scattered electrons and increase the number of electrons which eventually reach the detector. The vacuum value of $< \mathcal{O}(10^{-4})$ Pa was suggested by Lab Instructor Joe Piedle and was roughly confirmed by the electron counts during the experiment.

Both pumps were running 24 hours a day throughout the four weeks of the experiment in order to progressively reach the high vacuum needed for the most reliable results. This high vacuum ($< \mathcal{O}(10^{-4})$ Pa) was obtained by the end of week 2, and all the data presented in this paper comes from experimental rounds conducted after week 2.

F. Geiger-Mueller Detector

We measured electron counts in the experiment using a Geiger-mueller detector. Before any rounds of data collection, the voltage applied to the Geiger detector was tuned to lie in an optimal region where the counts per second registered by the counter were not only non-zero but were also independent of the applied voltage. Tuning the Geiger detector's applied voltage to be within this plateau ensured that small differences in applied voltage would not result in signal unrelated differences in Geiger counts. Thus after each day of the experiment, such small differences would not serve as anomalous signals in the data.

G. LABVIEW Program

We performed data collection using a LABVIEW program written by Joe Piedle. The program also controlled the high voltage applied to each capacitor plate and allowed us to sweep the voltage from 0 to 8 kV over a chosen interval of time. For such a sweep, the voltage stepped up from 0 to 8 kV over 200 increments in as many seconds. Having such a large number of steps, allowed us to achieve a high electron count per high voltage resolution in our data, but led to longer experimental run cycles.

With the program, we set a single round of data collection to perform five sweeps over which the counts for each sweep were aggregated until the end. Each channel corresponded to a particular voltage applied to the capacitor plates. By determining this voltage and knowing the distance between the plates, we found the electric field magnitude to which this potential difference corresponded with the formula

$$E = \frac{\Delta V}{d}, \tag{14}$$

where $\Delta V = V_+ - V_-$ is the potential difference between the positive and negative plates of the capacitor, and d is the distance between the plates. After each sweep, the LABVIEW output displayed the number of counts collected for each voltage channel. The signal peaks in the plots of the counts as a function of voltage channel are associated with electric field values where the electron counts are maximum. We in turn used this electric field value, the magnetic field value measured before each round of data collection, and Eq.(8) to determine the velocity of the electrons producing the signal.

IV. RESULTS AND ANALYSIS

Our electron count results obtained from LABVIEW are shown in Fig. 6a, where the counts have been normalized by dividing the total count seen in a channel by the average counts in the first 10 channels, which we took as background noise. Specifically, Fig. 6a displays, for various magnetic field values, how the number of electrons recorded by the Geiger detector varied as the voltage across the capacitor plates increased. The vertical axis in the figure corresponds to the number of counts, and

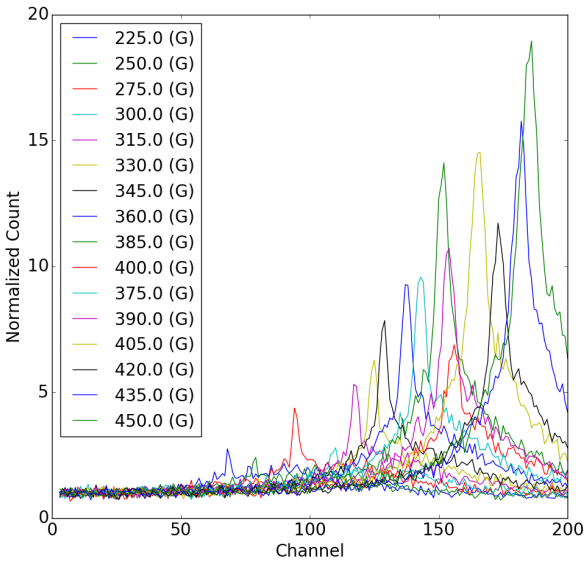

(a) Collected electron counts as a function of channel number for various magnetic fields. The uncertainty in the magnetic field was ±10 gauss. The channel number runs from 0 to 200 corresponding to an applied voltage from about 0 to 8 kV for the positive terminal and about 0 to -8 kV for the negative terminal of the capacitor plates. We note that the peak-to-background ratio for the electron counts increases as we increase the magnetic field as we should expect from Fig. 1

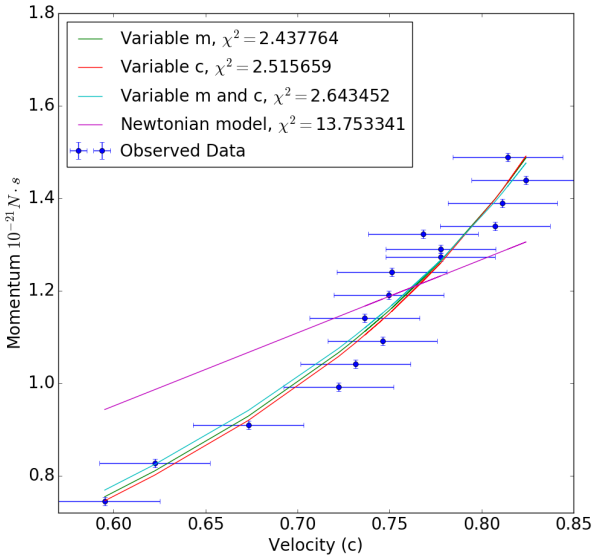

(b) Velocity and momentum measurements plotted for various fitting conditions with reduced-chi-squared values indicated for each fit. We note the relativistic fits (colored green, red, and light blue line) yield equations which fall within the uncertainty allowed by the data, the non -relativistic fit (colored magenta) lies well outside the data's range of uncertainty.

FIG. 6: Spectrometer results and momentum versus velocity fits.

the horizontal axis is the channel number running from 0 to 200 and corresponding to a voltage from 0 to $\sim \pm 8$ kV applied to each positive/negative capacitor plate. From the figure we see that each magnetic field measurement has a corresponding channel number associated with a peak in the electron count distribution. We determined this channel peak by locating the channel where the electron count distribution was highest.

After we determined the channel location of the peaks, we converted this channel location to an electric field prediction. Such an electric field defined a field value which allowed the greatest number of electrons to pass through the capacitor plates to the Geiger detector, and thus corresponded to an electric field yielding a zero net force on the electrons, that, is the electric field given in Eq.(7). With this electric field and the magnetic field previously measured, we then used Eq.(8) to determine the velocity of electrons which passed through the capacitor plates with the least deflection. Using our measured magnetic field, Eq.(13), and Eq.(5) we then determined the corresponding momentum of these electrons. In this way we collected velocity and momentum measurements for various magnetic fields.

Our collected velocity measurements are plotted against their corresponding momentum measurements in Fig. **??**. To obtain mass and speed of light predictions, we fit this data to Eq.(1) taking m alone, c alone, or both m and c together as fitting parameters. As a model comparison we also fit the data to the non-relativistic momentum formula [3]

$$p = mv \qquad \text{(Non-relativistic)}, \tag{15}$$

where m, the electron's mass, was the fitting parameter. We then used the `optimize.curvefit` [5] algorithm in Python's `scipy` package to implement the relativistic fits where c alone and both m and c were fitting parameters and employed `scipy.stats.linregress` [6] to implement the relativistic and non-relativistic fits where m alone was a fitting parameter. With these fits we also produced parameter predictions, and defined our errors as the square-root of the associated element in the covariance matrix.

In summary, the different conditions to which we fit our data were

1. Eq.(1) with m as fitting parameter
2. Eq.(1) with c as fitting parameter
3. Eq.(1) with m and c as fitting parameters

TABLE I: Electron mass and speed of light measurements: In the last row we list the current best known values of the electron mass and speed of light as given by [7].

Model/Fitting Params	m prediction (in 10^{-31} kg)	c prediction (in 10^8 m/s)
Rel./ m	9.3 ± 0.6	–
Rel./ c	–	2.96 ± 0.02
Rel./ m and c	9.5 ± 0.4	3.04 ± 0.09
NR./ m	0.144 ± 0.003	–
CRC Handbook values	9.10938291(40)	2.99792458

4. Eq.(15) with m as fitting parameter

In Table I, we collect the results of our parameter predictions as derived from our fits. We see that the accepted values of the electron mass and speed of light as given in [7] lie within the ranges predicted by our relativistic parameter fits. Moreover, the relativistic fits yield reduced-chi squared ([8]) values of ~ 2.5 suggesting they are acceptable fits. Conversely, the non-relativistic fit yields an electron mass prediction which does not encompass the current known value, and the corresponding reduced-chi squared value is much larger than 1 and hence suggests the fit is poor.

V. DISCUSSION

Across the four fitting schemes attempted on the velocity-momentum data, all three relativistic models performed significantly better than the Newtonian model. This can be seen in both the reduced χ^2 statistics for the four fits (as the Newtonian model produces a χ^2 statistic roughly an order of magnitude larger than the others) as well as in the plot of predicted and observed values. While all observed data fell within one standard error of the relativistic predictions, the Newtonian model predicted the results poorly and captured only 4 data points out of 16 within one standard error. Thus, we confirmed what we expected. First, Einstein's theory of special relativity better explains dynamical behavior at sufficiently high speeds. Second, we obtained results for the mass of the electron and the speed of light within 2% of the CRC value.

Among the relativistic models, only the model where m and c were both allowed to vary as fit parameters produced measurements of m and c within one standard error of the CRC values. This can be understood as a consequence of error propagation if we accept the CRC values of m and c as being better measurements of the "true" values. In fixing one of either m or c to the CRC, the other parameter had to capture the entirety of the deviations in the data from those obtained by the CRC model parameters.

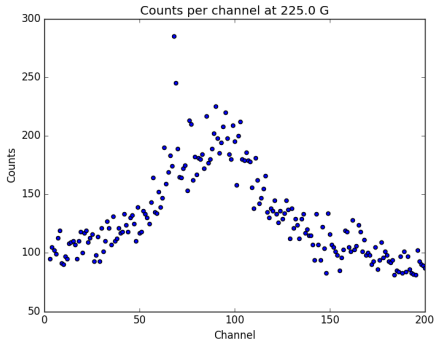

FIG. 7: Asymmetric counts with two peaks at 225G

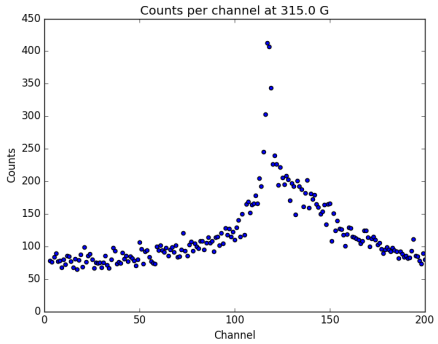

FIG. 8: Generally symmetric counts with one peak at 300G

One unexpected result was the asymmetry of the counts as we swept the voltage. In trials with high magnetic fields, usually above 300 gauss, the number of counts was generally symmetric, with slight skewing toward the left so that higher channels (higher voltages) tended to have somewhat higher counts (see Fig. 8). Below 300 gauss however, this discrepancy was much more noticeable. At 225 gauss (see Fig. 7), we even see two peaks with a very narrow peak near the 60th channel and a broad peak around the 100th channel. From three repeated trials below 225 gauss, the narrow peak at the 60th channel did not disappear, so we interpreted it as representing the channel corresponding to the actual condition where $E = vB$ given its strong signal-to-noise ratio and an extrapolation performed on peaks at higher magnetic fields.

One possible explanation for this asymmetry would be the finite rather than infinitesimal width of the spectrometer. In addition to increasing our variance by allowing electrons with velocities around but not exactly at $v = E/B$ to enter the Geiger detector and contribute to the counts, the geometry of our setup is such that having a finite width for our spectrometer introduces a preference for higher-velocity electrons over lower-velocity electrons around the selected velocity $v_s = E/B$. Consider an electron which has a velocity slightly less than v_s.

In the presence of the B field its radius of curvature is given by $R' = m(v_s - \delta v)/qB$ which will be less than $R_s = mv_s/qB$. Moreover, once the low-velocity electron enters the region of the electric field, its radius of curvature will only decrease, leading the electron to hit the sides of the spectrometer. Thus, the allowable deviation below v_s is small. Consider the allowable deviation at velocities above v_s. If the electron can enter the region of the electric field, then $E < (v_s + \delta v)B$. This yields the equations of motion

$$\ddot{x} = q(E + \dot{y}B)$$
$$\ddot{y} = -q\dot{x}B$$

Decoupling and solving the equations of motion, we see that the electron travels along a cycloid with its motion moving away from the nearest spectrometer wall. As it comes in with a radius of curvature larger than needed, if d is the width of the spectrometer, its allowable horizontal migration is at least $d/2$ while for the electron below velocity v it is less than $d/2$. Thus, each peak represents essentially the count $[v, v + \delta v]$. Given the spectrum of velocities emitted by Sr-90, at low B fields this has a significant impact on the distribution. That is, there are fewer low-velocity electrons to be filtered in the first place, yielding an asymmetry.

Other sources of error include the slightly above vacuum conditions of the spectrometer, which would reduce electron counts through collisions with air molecules. This would also bias the data as low-velocity electrons would be more affected by these collisions than high-velocity electrons. Finally, our results may have been systematically skewed by systematic biases in the voltage divider and gaussmeter.

VI. CONCLUSION

In this experiment we determined the speed of light and the mass of an electron by fitting spectrometric data to the relativistic formula for momentum in terms of velocity Eq.(1). Taking both m and c independently as fitting parameters we found $m = (9.3 \pm 0.6) \times 10^{-31}$ kg and $c = (2.96 \pm 0.2) \times 10^8$ m/s, the first of which encompasses the known electron mass of 9.109×10^{-31} kg and the second of which barely fails to encompass the known value of the speed of light 2.998×10^8 m/s.

In a larger sense, we demonstrated the superiority of the relativistic formula for momentum over the non-relativistic formula in velocity regimes where $v \sim \mathcal{O}(c)$, and thus affirmed one of the basic predictions of special relativity.

Acknowledgments

The authors are grateful to Joe Peidle for his assistance throughout the experiment. They are particularly appreciative of his early help in setting up the vacuum pumps and his constant monitoring of the vacuum needed to conduct the experiment.

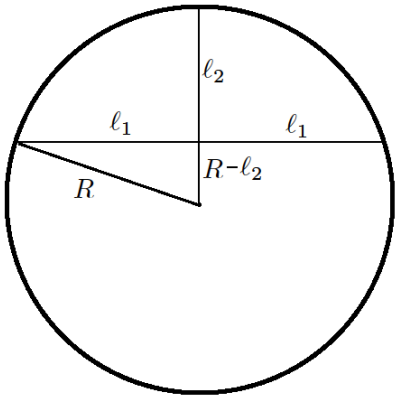

FIG. 9: Electron trajectory geometry: The full circle of the electron's trajectory implicit in Fig. 5.

Appendix A: Spectrometer Geometry

In this appendix we derive Eq.(13). As electrons leave the Sr-90 source in the spectrometer, they enter a magnetic field exclusive region where their trajectory comprises an arc of a circle as depicted in Fig. 5. The spectrometer diagram in Fig. 5 shows two lengths which characterize the geometry of this circle: $\ell_1 = 55.6$ mm which is half the length of a chord of the circle, and $\ell_2 = 47.6$ mm which runs from the edge of the circle to the chord and bisects it. We depict the full circle and these length definitions in Fig. 9. By the Pythagorean theorem we have

$$R^2 = \ell_1^2 + (R - \ell_2)^2, \tag{A1}$$

which upon solving for R leads to Eq.(13).

[1] E. Segrè, E. Segrè, and E. Segrè, *From x-rays to quarks: modern physicists and their discoveries*. WH Freeman San Francisco, 1980.

[2] S. S. Schweber, *QED and the men who made it: Dyson, Feynman, Schwinger, and Tomonaga*. Princeton University Press, 1994.

[3] D. Morin, *Introduction to classical mechanics: with problems and solutions*. Cambridge University Press, 2008.

[4] P. Horowitz, W. Hill, and T. C. Hayes, *The art of electronics*, vol. 2. Cambridge university press Cambridge, 1989.
[5] "scipy.optimize.curvefit," March 2016.
[6] "scipy.stats.linregress," April 2016.
[7] W. M. Haynes, *CRC handbook of chemistry and physics*. CRC press, 2014.
[8] P. R. Bevington and D. K. Robinson, "Data reduction and error analysis," *McGraw-Hill*, 2003.